Supporting Information

Fluorinated surface-to-bulk engineering enables high-rate and long-life sodium trititanate for sodium-ion batteries

Guangrong Zeng, Xin Jin, Fujie Li, Chao Wang*

Institute of Materials for Energy and Environment, College of Materials Science and Engineering, Qingdao University, Qingdao 266071, P. R. China

*Corresponding author and email address: wangc@qdu.edu.cn (CW)

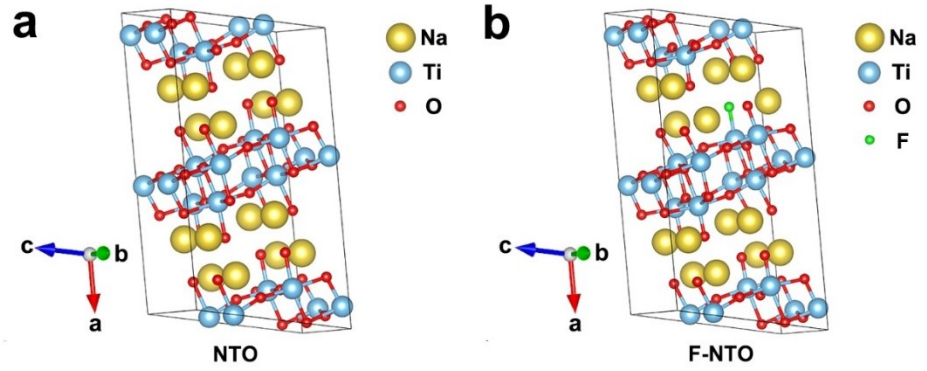

Fig. S1. The specific computational models employed for NTO (a) and F-NTO (b)in the DFT calculations.

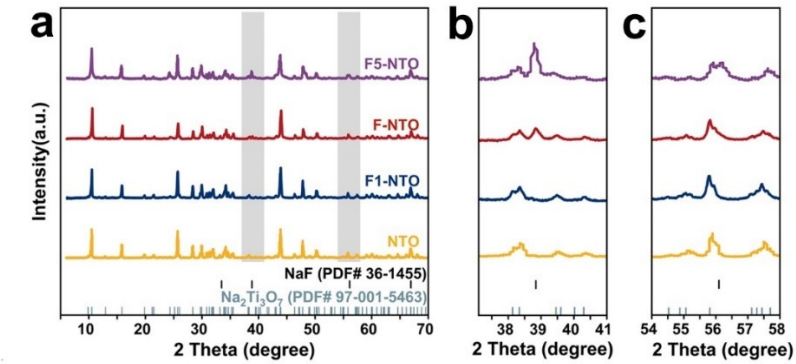

Fig. S2. XRD patterns of NTO, F1-NTO, F-NTO, and F5-NTO (a), along with their corresponding enlarged views (b, c).

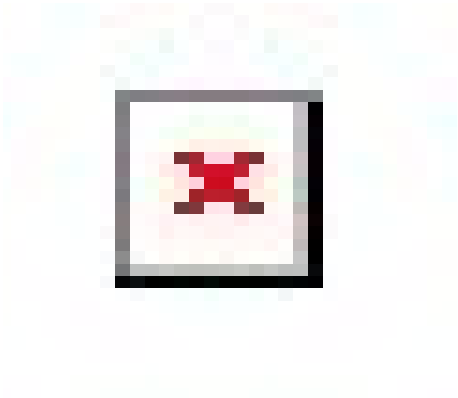

Fig. S3. Rietveld refinement of the XRD patterns for NTO.

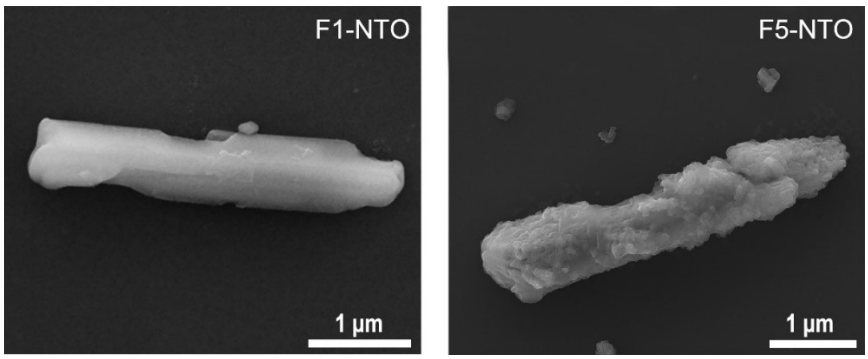

Fig. S4. FESEM images of F1-NTO (a) and F5-NTO (b).

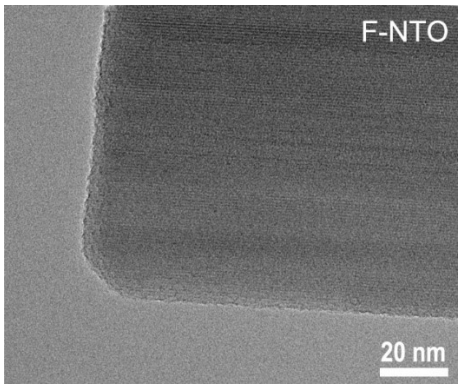

Fig. S5. TEM image of F-NTO.

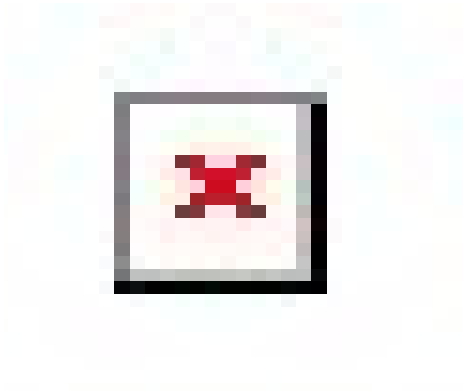
Fig. S6. XPS survey spectra of NTO and F-NTO.

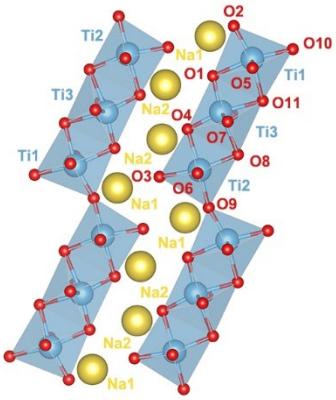

Fig. S7. Crystal structures of NTO showing the locations of different atoms.

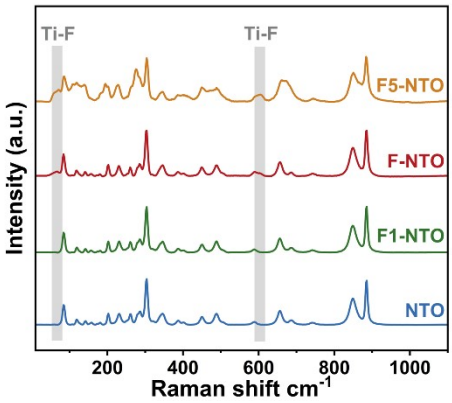

Fig. S8. Raman spectra of NTO, F1-NTO, F-NTO and F5-NTO.

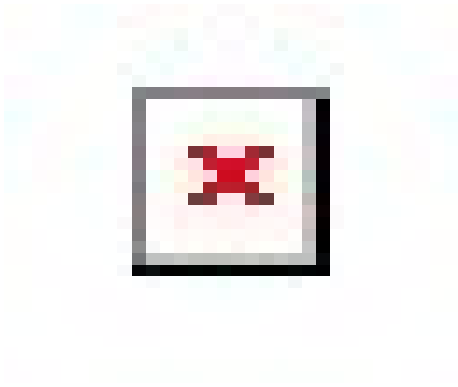

Fig. S9. The first 10 CV curves of NTO at 0.1 mV s^{-1}.

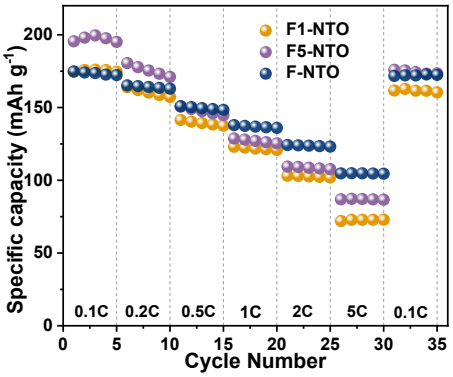

Fig. S10. Rate performance of F1-NTO, F-NTO and F5-NTO.

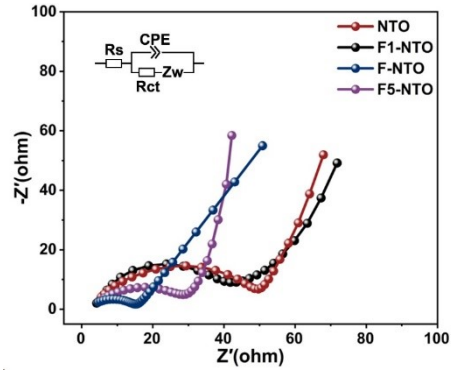

Fig. S11. Nyquist plots of NTO, F1-NTO, F-NTO and F5-NTO before cycling.

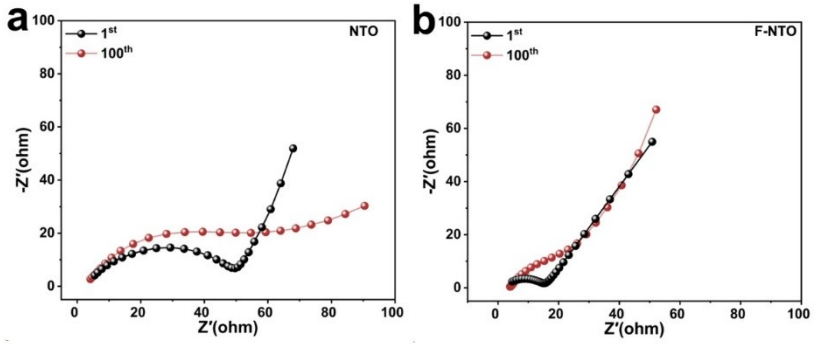

Fig. S12. Nyquist plots of NTO (a) and F-NTO (b) electrodes before and after 100 cycles.

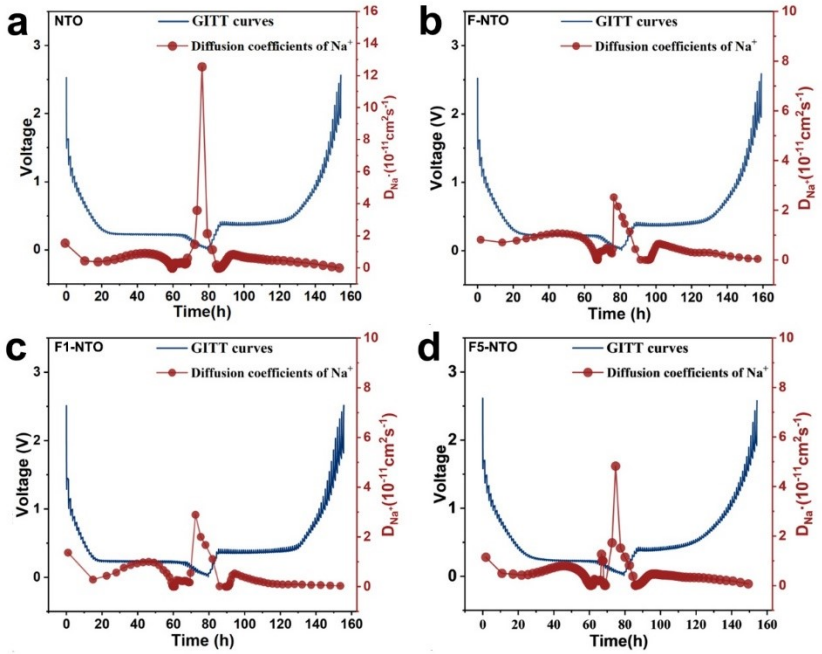

Fig. S13. GITT curves (blue) and variations in apparent Na^+ diffusion coefficients (red) of NTO (a), F-NTO (b), F1-NTO (c) and F5-NTO (d).

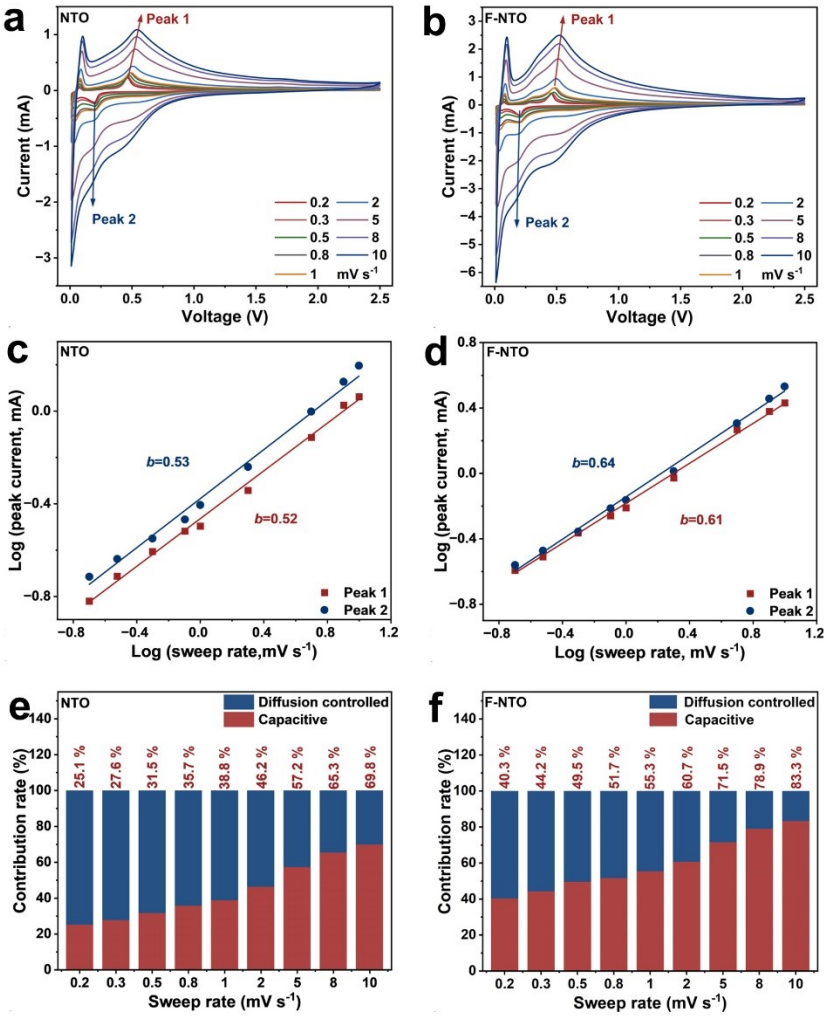

Fig. S14. CV curves of NTO (a) and F-NTO (b) at different sweep rates; *b* values for anodic and cathodic peaks of NTO (c) and F-NTO (d); diffusion-controlled and capacitive contributions to Na^+ storage at different sweep rates for NTO (e) and F-NTO (f).

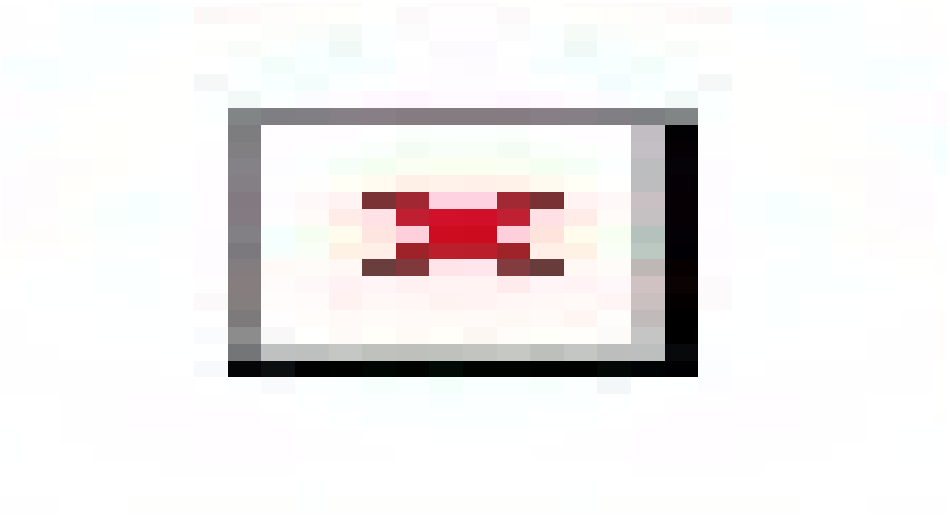

Fig. S15. Contour plots of in situ XRD data of NTO during the first cycle.

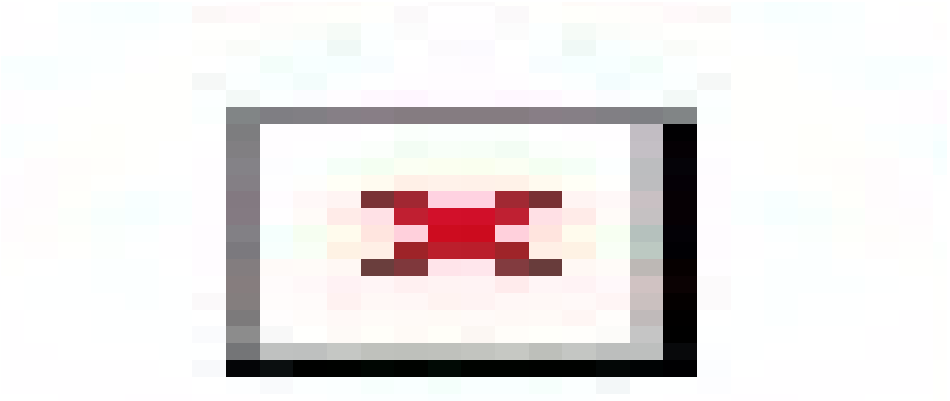

Fig. S16. Contour plots of in situ XRD data of F-NTO during the first cycle.

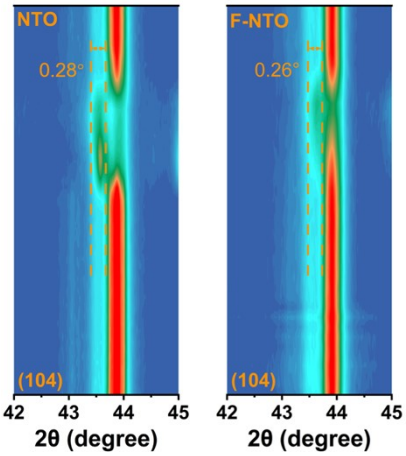

Fig. S17. In situ XRD patterns of NTO and F-NTO during the initial cycle in the region of the (104) diffraction peak.

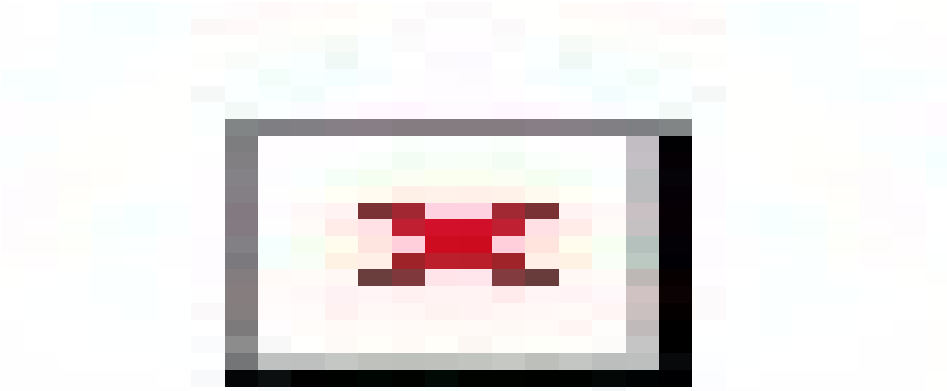

Fig. S18. In situ Raman contour plots of NTO during the first cycle. The left panel shows the corresponding discharge-charge profile during the first cycle.

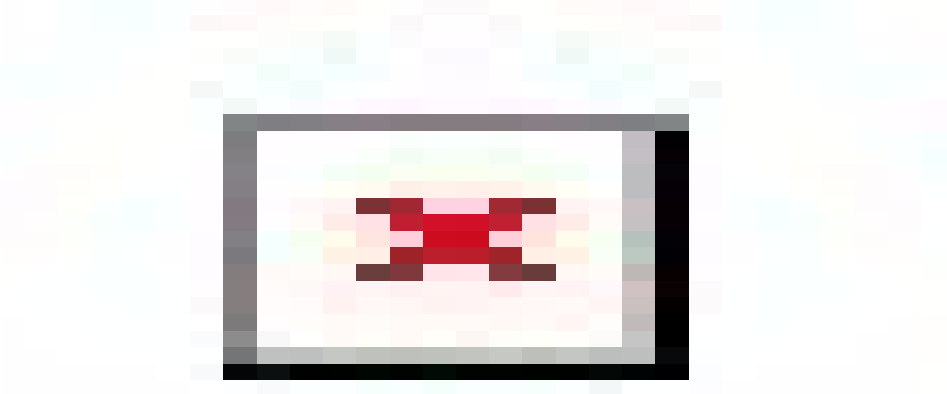

Fig. S19. In situ Raman contour plots of F-NTO during the first cycle. The left panel shows the corresponding discharge-charge profile during the first cycle.

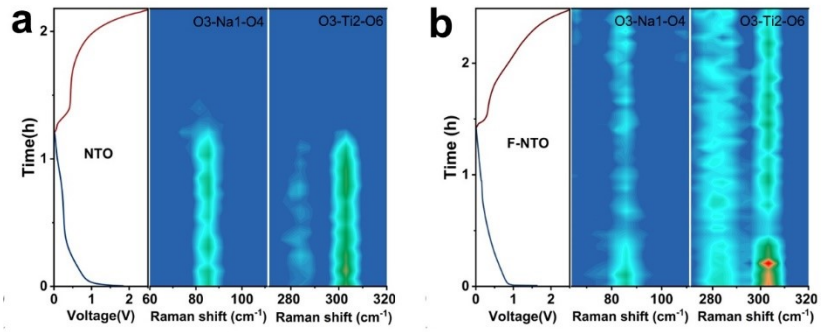

Fig. S20. In situ Raman contour plots of NTO (a) and F-NTO (b) during the initial cycle with selected regions of the O3-Na1-O4 and O3-Ti2-O6 peaks.

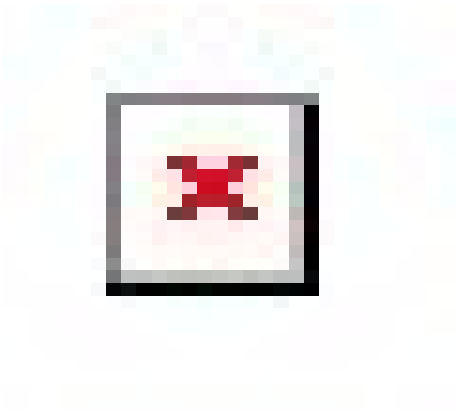

Fig. S21. Raman spectra of NTO and F-NTO after 100 cycles.

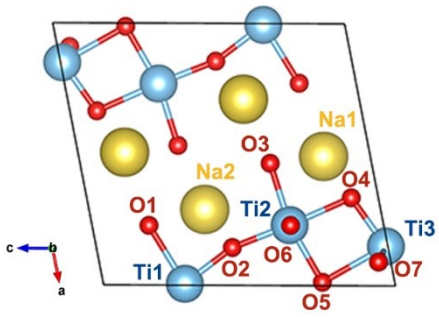

Fig. S22. Crystal structure of $Na_2Ti_3O_7$ showing different O atom positions.

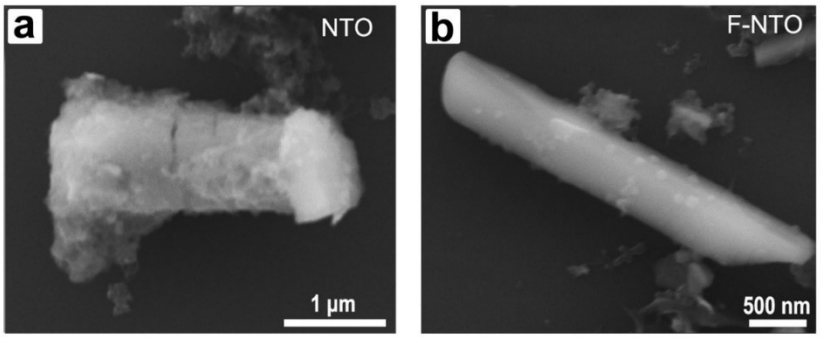

Fig. S23. FESEM images of NTO (a) and F-NTO (b) after 100 cycles.

Table S1. Rietveld refinement results of XRD data for NTO, F1-NTO, F-NTO, and F5-NTO.

Sample	*a* (Å)	*b* (Å)	*c* (Å)	*V* (Å^3)
NTO	8.565	3.802	9.129	291.238
F-NTO	8.574	3.803	9.132	291.764

Table S2. The summarization of peak position and corresponding compounds ratio in Ti2*p*.

Peaks	Positions (eV)	Ratio (%)		
		0 s	60 s	120 s
$Ti^{3+}2p_{3/2}$	456.6	16.1	11.5	8.6
$Ti^{3+}2p_{1/2}$	461.8	8.0	5.7	4.3
$Ti^{4+}2p_{3/2}$	458.5	50.6	55.2	29.0
$Ti^{4+}2p_{1/2}$	464.2	25.3	27.6	58.1

Table S3. The summarization of peak position and corresponding compounds ratio in O1*s*.

Peaks	Positions (eV)	Ratio (%)		
		0 s	60 s	120 s
C-O	533.5	9.4	9.4	5.2
C=O	531.1	48.8	37.2	28.7
Ti-O	529.3	36.5	48.3	62.1
Na KLL Auger	535.8	5.3	5.1	4.0

Table S4. The summarization of peak position and corresponding compounds ratio in F1*s*.

Peaks	Positions (eV)	Ratio (%)		
		0 s	60 s	120 s
Ti-F	684.9	66.7	100	100
NaF	684	33.3	-	-

Table S5. Experimental Raman shift assignments of NTO and F-NTO.

Exp. (cm^{-1})		Assignment	Exp. (cm^{-1})		Assignment
NTO	F-NTO		NTO	F-NTO	
85	85	αNa1	319	319	δ_aO4-Ti1-O5
107	107	αNa2, Ti2	345	345	δ_aO4-Ti1-O5
121	121	αNa2	387	387	δ_aO6-Ti3-O7
142	142	ρO2-Ti2-O3	401	401	υ_sO4-Ti2-O5
156	156	αNa2	450	450	σO5-Ti1-O4
174	174	αNa2	489	489	υ_aTi2-O6
181	181	τO4-Ti2-O5	506	506	υTi1-O7
202	202	τO1-Ti3-O2	588	588	υ_aTi1-O7
230	230	δ_aNa1-O3	655	655	υ_aTi2-O10
261	261	τTi1-O1-Ti3	684	684	δ_aO4-Ti1-O1
280	280	τO5-Ti2-O6	742	742	υ_sO1-Ti1-O4
284	284	ωO3-Ti2-O4	848	848	υTi1-O4
304	304	ωO2-Ti2-O6	885	885	υ_sO3-Ti2-O5

Note: υ for bond stretching, δ for deformation, ω for wagging, σ for scissoring, τ for twisting, ρ for rocking, and α for a complex lattice mode. The *s* and *a* subscripts denote symmetric and antisymmetric movements, respectively.

Table S6. The fitted values of R_s and R_{ct} of NTO, F1-NTO, F-NTO and F5-NTO using the equivalent circuit model.

Sample	Initial		After 100 cycles	
	R_s (Ω)	R_{ct} (Ω)	R_s (Ω)	R_{ct} (Ω)
NTO	3.0	43.5	2.5	70.8
F1-NTO	3.8	35.3	-	-
F-NTO	1.9	13.9	4.0	32.3
F5-NTO	2.3	33.2	-	-

Table S7. Diffusion coefficients of Na^+ of NTO, F1-NTO, F-NTO and F5-NTO.

D_{Na+} ($\times 10^{-12}$ cm^2 S^{-1})	Discharge	Charge
NTO	1.23	1.43
F1-NTO	2.10	1.71
F-NTO	3.33	3.19
F5-NTO	2.86	2.98

Table S8. The summarization of peak position and corresponding compounds ratio in C1s after 100 cycles.

Peaks	Positions (eV)	Ratio (%)					
		NTO			F-NTO		
		0 s	60 s	120 s	0 s	60 s	120 s
O─C═O	289.5	7.0	14.9	14.0	1.0	4.2	3.5
RCH_2–F	288.6	17.4	17.8	12.6	10.7	0.0	0.0
C═O	287.8	13.0	13.3	16.8	8.8	10.9	10.1
C─O	286	4.4	10.8	13.5	9.4	16.1	10.6
C─C	284.6	52.3	35.1	34.3	38.1	47.0	51.6
C─Ti	282.7	5.9	8.1	8.8	32.0	21.8	24.2

Table S9. The summarization of peak position and corresponding compounds ratio in O1s after 100 cycles.

Peaks	Positions (eV)	Ratio (%)					
		NTO			F-NTO		
		0 s	60 s	120 s	0 s	60 s	120 s
Na KLL Aguer	535.8	25.5	21.1	20.8	11.0	15.8	17.3
C—O	533.5	14.0	19.5	19.3	28.6	24.6	23.1
C═O	531.1	47.2	35.6	32.0	19.5	21.6	24.1
Ti—O	529.6	13.3	23.8	27.9	40.9	37.9	35.5

Table S10. The summarization of peak position and corresponding compounds ratio in F1s after 100 cycles.

Peaks	Positions (eV)	Ratio (%)					
		NTO			F-NTO		
		0 s	60 s	120 s	0 s	60 s	120 s
F-P	687.3	46.5	6.4	4.8	12.9	-	-
Ti-F	684.9	-	-	-	23.9	18.4	18.6
NaF	683.7	53.5	93.6	95.2	63.2	81.6	81.4

Table S11. The summarization of peak position and corresponding compounds ratio in Ti2*p* after 100 cycles.

Peaks	Positions (eV)	Ratio (%)					
		NTO			F-NTO		
		0 s	60 s	120 s	0 s	60 s	120 s
Ti$2p_{3/2}$	453.7	37.7	27.5	26.1	-	-	-
Ti$2p_{1/2}$	459.8	18.8	13.8	13.1	-	-	-
$Ti^{3+}2p_{3/2}$	456.6	29.0	39.2	40.5	57.1	43.6	36.9
$Ti^{3+}2p_{1/2}$	461.8	14.5	19.6	20.3	28.5	21.8	18.4
$Ti^{4+}2p_{3/2}$	458.5	-	-	-	9.6	23.1	29.8
$Ti^{4+}2p_{1/2}$	464.2	-	-	-	4.8	11.5	14.9